values fall on or near the turbulent correlation line. At the two lower Reynolds numbers there are some data points for the rougher walls that are noticeably above the correlation line. At Mach 4.4 (Fig. 3d), the highest Mach number reached in this study, the heat-transfer values either fall on the correlation line or at the lower Reynolds numbers appreciably above it. In Ref. 2, among others, it is shown that the boundary layer thins down upstream of the throat, reaches a minimum near the throat, and then proceeds to thicken downstream of the throat. At Mach 3.75 and 4.4, the boundary layer is much thicker than it would be at the throat and consequently the same holds true for the sublayer height. In the vicinity of the throat the higher values of surface roughness protrude through the sublayer and cause a heat transfer increase (Ref. 5). However, in the high Reynolds number region of the two high Mach number cases all the roughness heights are contained within the thick sublayer and consequently roughness does not affect the heat transfer. Those data points indicated by the solid symbols represent flow separation which was determined by the fluctuations in the static pressure. Other than indicating that separation has taken place, the data points represented by the solid symbols have no meaning in Figs. 3c and d.

In order to get an over-all picture of roughness effects on heat transfer in the supersonic region of a conical nozzle let us again look at Fig. 1. The scope of this Note is the region where the acceleration decreases and the pressure gradient becomes less favorable. Mach 3.75 and 4.4 are in a region where the favorable pressure gradient is very small, less than $\frac{1}{2}$ of 1% of maximum. One would expect the heat transfer at these Mach numbers to behave as they would under a zero pressure gradient. The results shown in Fig. 3 bear this out for those points not undergoing separation. The heat-transfer parameters compare very favorably with the turbulent correlation. There is no laminarization or detransition. The roughness values used in this Note do not affect the heat transfer which is probably due to a thick boundary layer resulting from the negligible pressure gradient.

At Mach 1.71 and 2.12 the acceleration and favorable pressure gradient are relatively high, but they are less than their respective maxima and dropping off very fast. The resulting heat transfer has some of the characteristics of the maximum acceleration (Fig. 2) but to a lesser degree. Although roughness still affects the heat transfer because the boundary layer has not yet become very thick, there is less evidence of detransition and hardly any of laminarization, two major characteristics of highly accelerated flow.

References

[1] Boldman, D. R., Neumann, H. E., and Schmidt, J. F., "Heat Transfer in 30° and 60° Half-Angle of Convergence Nozzles with Various Diameter Uncooled Pipe Inlets," TN D-4177, 1967, NASA.

[2] Graham, R. W. and Boldman, D. R., "The Use of Energy Thickness in Prediction of Throat Heat-Transfer in Rocket Nozzles," TN D-5356, 1969, NASA.

[3] Back, L. H., Massier, P. F., and Cuffel, R. F., "Flow Phenomena and Convection Heat Transfer in a Concial Supersonic Nozzle," *Journal of Spacecraft and Rockets*, Vol. 4, No. 8, Aug. 1967, pp. 1040–1047.

[4] Boldman, D. R., Schmidt, J. F., and Gallagher, A. K., "Laminarization of a Turbulent Boundary Layer as Observed from Heat-Transfer and Boundary-Layer Measurements in Conical Nozzles," TN D-4788, 1968, NASA.

[5] Reshotko, M., Boldman, D. R., and Ehlers, R. C., "Heat-Transfer in a 60° Half-Angle of Convergence Nozzle with Various Degrees of Roughness," TN D-5887, 1970, NASA.

[6] Reshotko, M., Boldman, D. R., and Ehlers, R. C., "Effects of Roughness on Heat Transfer in Conical Nozzles," *Augmentation of Convective Heat and Mass Transfer*, ASME, 1970.

Spin Rate Behavior of ISIS-I

F. R. VIGNERON,* D. HARRISON,† AND G. BOWER‡
Communications Research Center, Ottawa, Canada

Nomenclature

$\mathbf{B}$ = Earth's magnetic field vector
$\bar{B}^2$ = time average over an orbit of the square of the component of the Earth's field resolved on a normal to the satellite spin axis
C = moment of inertia, 7.7312×10^9 g-cm^2
p = eddy current damping resistivity constant
s = spin rate
t = time
T = torque
$\mathbf{V}$ = satellite orbital velocity

THE spin rate behavior of ionospheric sounding satellites with long flexible antennas in crossed dipole configuration has been of continuing interest since the launch of Alouette I in 1962.[1] Flight data from Alouette I and Explorer XX show a slow decay of spin rate, which may be attributed mainly to a 'solar motoring torque' resulting from an interaction between the solar pressure field and the flexible antennas.[2–4] This Note discusses spin rate data obtained from the ISIS-I[5] ionospheric sounding satellite launched in 1969, in the light of solar motoring and other possible despin torque mechanisms.

Measured spin rate data of ISIS-I taken from date of launch to July of 1970 are shown in Fig. 1. In general, the characteristic slow decay of spin rate is observed. Discontinuities in spin rate on days 91, 97, 243 and so forth, result from the operation of the ISIS control system.[6] Also shown on Fig. 1 are the percent sun variation and the measured variation of solar aspect angle (the angle between the spin axis and the sun line). The measured right ascension and codeclination of the spin axis are presented in Fig. 2.

The data between attitude maneuvers of days 100 and 243 of 1969 shows a period of high despin in the neighborhood of day 160 (Fig. 1). A fifth-order polynomial least-squares fit is found to provide an acceptable analytical model over the 143 day interval, as shown in Fig. 3. A torque history con-

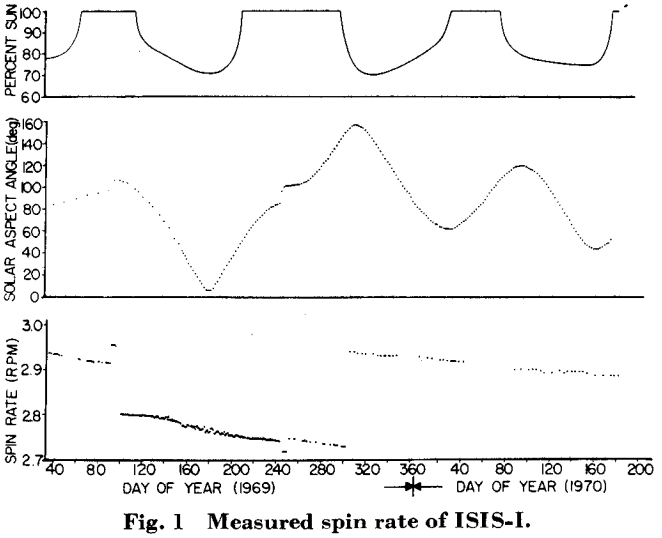

Fig. 1 Measured spin rate of ISIS-I.

Received February 24, 1971; revision received May 27, 1971. Index category: Spacecraft Attitude Dynamics and Control.

* Research Scientist. Member AIAA.
† Engineer, Space Mechanics Section.
‡ Electronics Technician, Space Mechanics Section.

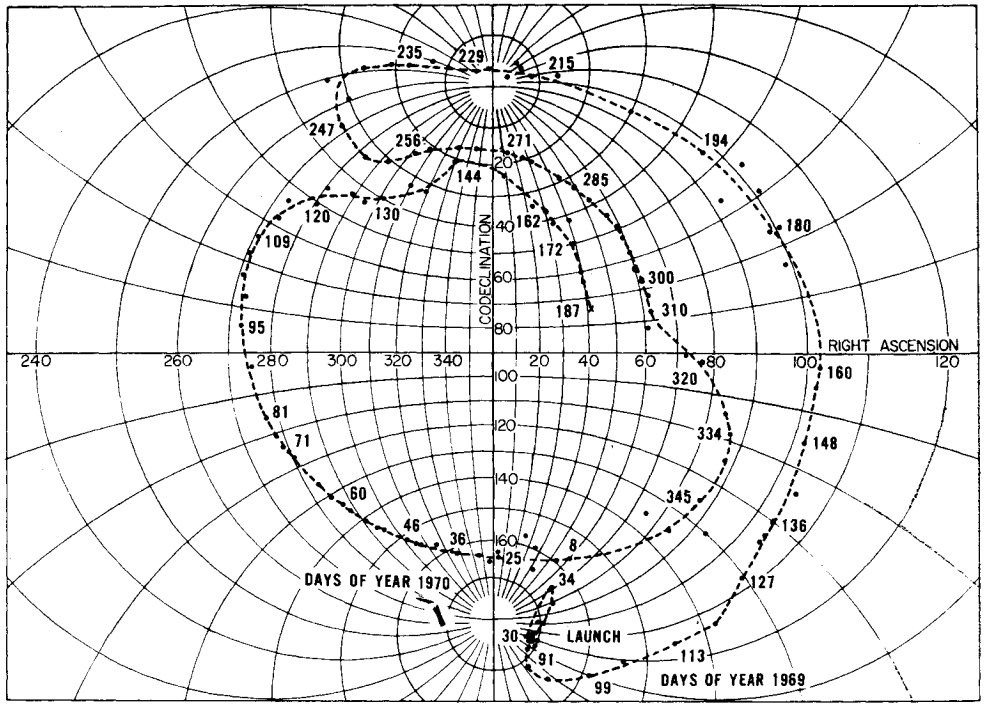

Fig. 2 Spin vector motion of ISIS-I.

structed from the fifth-order polynomial by the formula

$$T = C\, ds/dt \tag{1}$$

reveals torque to be negative in sign and 1–7 dyne-cm in magnitude. The torque curve shown in Fig. 3 compares well with curves based on fourth and sixth order polynomial fits.

The performance of earlier sounding satellites leads one to anticipate that the observed despin would be attributable mainly to solar motoring.[2,4] The theory of Ref. 2 predicts, for ISIS-I, a torque negative in sign and possibly of the correct order of magnitude. In the present case, however, the percent sun is minimum and the solar aspect angle is virtually zero (Fig. 1) during the time of highest despin action, thus ruling out the solar motoring as the principal torque mechanism (although its contribution to the torque at other times may be significant). For the same reasons aerodynamic torques[7] may be discounted in importance.

On day 160, ISIS-I's orbital perigee was over the Earth's South Pole with a line of apsides drift of 1.99° per day and its spin vector aligned approximately perpendicular to the Earth's axis (codeclination of about 90°, Fig. 2). This configuration is well-suited for electrodynamic interaction between the satellite and the Earth's magnetic field. Periods of increased despin activity discernable in the neighborhood of days 314, 1969 and 15, 1970, likewise may be correlated with a configuration favorable for electrodynamic interaction.

Eddy current and magnetic hysteresis damping, effects well-demonstrated on previous flights,[8–10] are possible despin mechanisms of significance as the structure is composed of an aluminium honeycomb outer skin with 8 internal ribs which effectively form four conducting coils normal to the satellite spin axis. An expression for average eddy current torque generated over an orbit is[10]

$$T = -ps\bar{B}^2 \tag{2}$$

Magnetic hysteresis torques[9] are also approximately proportional to $\bar{B}^2$. The $\bar{B}^2$ function may be calculated to within a few percent from a theoretical field model, the spin vector information of Fig. 2, and the known orbital ephemeris of the satellite. A least-squares fit of Eq. (2) (with $\bar{B}^2$ and s as known functions) to the torque curve of Fig. 3 then yields value of p of 17.8 dyne-cm-sec/moe^2. Although the value of p is virtually impossible to calculate satisfactorily by analytical means because of the complex satellite geometry, the best estimates are compatible with the 17.8 value. The fitted curve falls short of matching the measured data in shape as is noted in Fig. 4. Inclusion of any amount of solar motoring makes the fit even poorer. Hence this strongly suggests that eddy current and magnetic hysteresis damping do not account fully for the measured despin action.

Concluding Remarks

Assessment of order of magnitude of other recognized spin axis torques reveals two that may be of significance for ISIS satellites: 1) ion impact torque (Coloumb torque)[11–13]—a $\mathbf{V} \times \mathbf{B}$ induced potential across the dipole antenna,[5,14] being

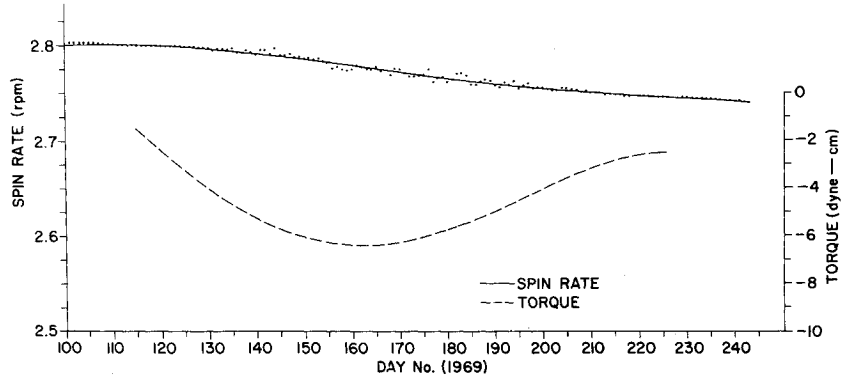

Fig. 3 Fifth-order polynomial fit of spin rate and resulting torque curve.

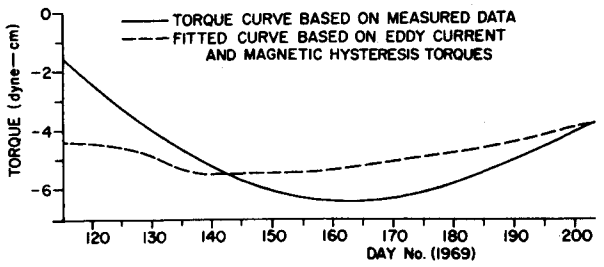

Fig. 4 Fitted torque curve.

symmetric with respect to the satellite mass center, causes the net bombardment of charged ions of the ionosphere to impact with an unsymmetrical distribution, therefore, causing a torque; 2) torque from $\mathbf{V} \times \mathbf{B}$ induced current (induction torque)[11]—a $\mathbf{V} \times \mathbf{B}$ induced potential across the dipole antenna results in a flow of electrons along the antenna,[14] which in turn interacts with the Earth's magnetic field to produce an electrostatic force and consequently a torque. The $\mathbf{V} \times \mathbf{B}$ potential distribution is dependent on photoemission,[11,14] and consequently the resulting torques have a dependence on percent sun (Fig. 1).

Several combinations of the previously discussed torques may be conjectured as the cause of the anomalous measured torque history. The quality and amount of measured dynamics data on ISIS-I does not permit the various mechanisms to be isolated and conclusively identified at this point.

References

[1] Paghis, I., Franklin, C. A., and Mar, J., "Alouette I, The First Three Years in Orbit," DRTE Rept. 1169, March 1967, Dept. of National Defence, Ottawa, Canada.

[2] Etkin, B. and Hughes, P. C., "Explanation of the Anomalous Spin Behavior of Satellites with Long Flexible Antennas," *Journal of Spacecraft and Rockets*, Vol. 4, No. 9, Sept. 1967, pp. 1139–1145.

[3] Mar, J. and Garrett, T., "Mechanical Design and Dynamics of the Alouette Spacecraft" *Proceedings of the IEEE*, Vol. 57, No. 6, June 1969, pp. 882–896.

[4] Hughes, P. C. and Cherchas, D. B., "Spin Decay of Explorer XX," *Journal of Spacecraft and Rockets*, Vol. 7, No. 1, Jan. 1970, pp. 92–93.

[5] Florida, C. D., "The ISIS Series of Ionospheric Satellites," *Proceedings of the Eighth International Symposium on Space Technology and Science*, Tokyo, 1969, AGNE Publishing, Japan, pp. 1073–1087.

[6] Kowalik, H., "A Spin and Attitude Control System for the ISIS-I and ISIS-B Satellites," *Automatica*, Vol. 6, 1970, pp. 673–682.

[7] Vigneron, F. R. and Garrett, T. W., "Solar Induced Distortion—Atmospheric Drag Coupling in Alouette Satellites," DRTE Rept. 1171, Feb. 1967, Dept. of National Defence, Ottawa, Canada.

[8] Wilson, R. A., "Rotational Magnetodynamics and Steering of Space Vehicles," TN D-566, Sept. 1961, NASA.

[9] Fischell, R. E., "Magnetic Damping of the Angular Motions of Earth Satellites," *American Rocket Society Journal*, Vol. 31, No. 9, Sept. 1961, pp. 911–913.

[10] Yu, Y. E., "Spin Decay, Spin-Precession Damping, and Spin Axis Drift of the Telestar Satellite," *Bell System Technical Journal*, Vol. 42, Sept. 1963, pp. 2169–2193.

[11] Wood, G. P. and Hohl, F., "Electric Potentials, Forces, and Torques on Bodies Moving Through Rarefied Plasmas," *Proceedings of the AIAA and Northwestern University 6th Biennial Gas Dynamics Symposium*, Evanston, Ill., Aug. 25–27, 1965.

[12] Hohl, F. and Wood, G. P., "The Electrostatic and Electromagnetic Drag Forces on a Spherical Satellite in a Rarefied, Partially Ionized Atmosphere," *Rarefied Gas Dynamics*, Academic Press, New York, 1963, pp. 45–64.

[13] Brundlin, C. L., "Effects of Charged Particles on the Motion of an Earth Satellite," *AIAA Journal*, Vol. 1, No. 11, Nov. 1963, pp. 2529–2538.

[14] Kasha, M., *The Ionosphere and Its Interaction With Satellites*, Gordon and Breach, New York, 1969, Chap. 5.

Injection into a Supersonic Stream from the Windward Side of Sweptback Injectors at Angle of Attack

M. Hersch* and L. A. Povinelli†

NASA Lewis Research Center, Cleveland, Ohio

It has previously been shown[1–3] that vortices, generated by delta wing injectors at an angle of attack, can enhance penetration and mixing of a secondary jet into a supersonic stream. In these previous studies helium was injected at sonic velocity normal to the leeward side of the injectors directly into the vortex region. Although penetration and mixing were improved in comparison to injection from a flat plate in a vortex free flowfield, two problems were noted. Firstly, a significant portion of the jet was not captured by the vortex, but flowed directly downstream as if injected from a flat plate in a vortex free flowfield.[2] Secondly, the jet appeared to disrupt the vortex motion.[3] These problems might be overcome by matching the direction and velocity of the jet to the vortex.

An alternate injection technique is suggested by the fact that the leeward vortex originates from flow which sweeps over the leading edge from the windward side of the wing.[4] It might be anticipated then, that injectant from the windward side would be carried by this flow into the leeward vortex. Also, disruption of the vortex might be minimized if the injectant were introduced at a low velocity distributed over a large area. This might be accomplished by injecting the gas from a porous surface as opposed to discrete orifices. In this study two injectors were tested to explore these ideas (Figs. 1 and 2).

One injector, configuration A (Fig. 1), had a single sharp leading edge sweptback at 58.5°. This injector may be

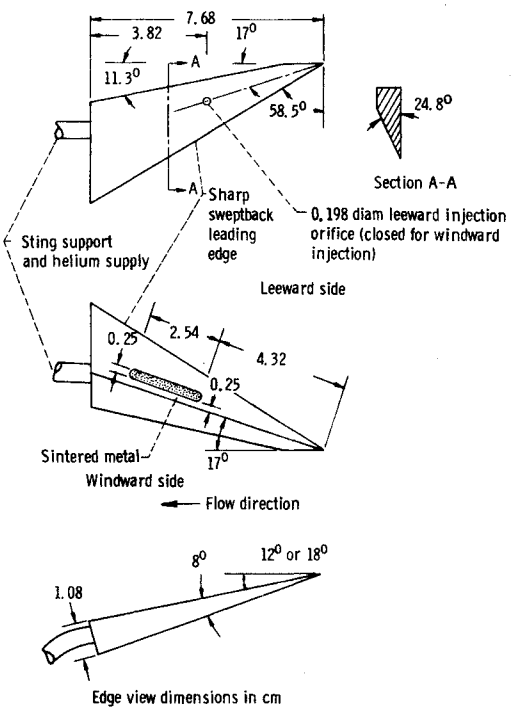

Fig. 1 Injector configuration A.

Received June 24, 1971.

* Aerospace Research Scientist, Hypersonic Propulsion Section.

† Aerospace Research Scientist, Hypersonic Propulsion Section. Associate Fellow AIAA.